Fire-precipitation interactions amplify the quasi-biennial variability of fires over southern Mexico and Central America

Yawen Liu [1, 2], Yun Qian [3*], Philip J. Rasch [3*], Kai Zhang [3], L. Ruby Leung[3], Yuhang Wang [4], Minghuai Wang [1, 2], Hailong Wang [3], Xin Huang[1,2], and Xiu-Qun Yang [1]

[1]School of Atmospheric Sciences, Nanjing University, China

[2]Joint International Research Laboratory of Atmospheric and Earth System Sciences & Institute for Climate and Global Change Research, Nanjing University, China

[3]Pacific Northwest National Laboratory, Richland, Washington, USA

[4]School of Earth and Atmospheric Sciences, Georgia Institute of Technology, Atlanta, Georgia, USA

Correspondence to: Yun Qian and Philip J Rasch and (yun.qian@pnnl.gov and Philip.Rasch@pnnl.gov)

Abstract. Fires have great ecological, social, and economic impacts. However, fire prediction and management remain a challenge due to a limited understanding of their role in the Earth system. Fires over southern Mexico and Central America (SMCA) are a good example, which greatly impact local air quality and regional climate. Here we report that the spring-peak (Apr-May) fire activities in this region have a distinct quasi-biennial signal based on multiple satellite datasets measuring different fire characteristics. The variability is initially driven by the quasi-biennial variations of precipitation. Composite analysis indicates that strong fire years correspond to suppressed ascending motions and weakened precipitation over the SMCA. The anomalous precipitation over the SMCA is further found to be mostly related to the East Pacific-North Pacific (EP-NP) pattern two months previous to the fire season. The positive phase of EP-NP leads to enhanced precipitation over the eastern US yet suppressed precipitation over SMCA, similar to the spatial pattern of precipitation difference between strong and weak fire years. Meanwhile, the quasi-biennial signals in precipitation and fires appear to be amplified by their interactions through a positive feedback loop on short timescales. Model simulations show that in strong fire years, more aerosol particles are released and transported downstream over the Gulf of Mexico and the eastern US, where suspended light-absorbing aerosols warm the atmosphere and cause ascending motions of the air aloft. Subsequently, a compensating downward motion is formed over the fire source region and ultimately suppresses precipitation and intensifies fires. Statistical analysis shows the different duration of the two-way interaction, where the fire suppression effect by precipitation lasts for more than 20 days, while fire leads to a decrease in precipitation at shorter time scales (3-5 days). This study demonstrates the importance of fire-climate interactions in shaping the fire activities on interannual scale and highlights how precipitation-fire interactions at short timescales contribute to the interannual variability of both fire and precipitation.

1 Introduction

Natural and human-induced fires are key features of the Earth system (Bowman et al., 2009). Uncontrolled large fires damage biodiversity, affect human health, and incur high economic costs (Knorr et al., 2017; Aguilera et al., 2021; Bowman et al., 2017). Comprehensive knowledge of fires' causes, variability, and climate effects is necessary to accommodate or manage fires effectively, and to mitigate adverse societal impacts.

Changes in climate alter fire regimes (Power et al., 2008; Jolly et al., 2015), because the occurrence and intensity of fires depend on meteorological factors such as precipitation, wind, and humidity (Flannigan et al., 2009; Marlon et al., 2008; Abram et al., 2021; Fang et al., 2021). Fires alter weather and climate as well: they are important sources of aerosol particles that modify Earth's energy and water budget either by directly absorbing and scattering sunlight or affecting cloud microphysical processes (Voulgarakis and Field, 2015; Jiang et al., 2020; Liu et al., 2018; Yue et al., 2022; Lu et al., 2018). There are many modes of interaction. The modes are complex, operate through a variety of mechanisms, and manifest on a large variety of time and space scales (Ding et al., 2021; Zhang et al., 2022). For example, Huang et al. (2023) have demonstrated that synoptic-scale fire-weather feedback plays a prime role in driving extreme fires in the Mediterranean and monsoon climate regimes over the US West Coast and Southeastern Asia. On interannual scales, fires in the maritime subcontinent have been shown to affect SSTs, land temperature as well as atmospheric stability, and influence ENSO on 3-6 year timescales (Tosca et al., 2010). The extreme 2019-2020 Australian fires have also been demonstrated to contribute to the 2020-2022 strong La Niña event by enhancing cloud albedo, cooling and drying out the air, and forming a positive feedback between the northward migration of intertropical convergence zone and sea surface temperature cooling in the Niño3.4 region (Fasullo et al., 2023). Moreover, on even longer timescales, fires can affect the accumulation of carbon dioxide and methane by modifying global features like the Hadley circulation that change precipitation and temperature patterns and eventually affect forest ecosystems to produce feedback operating over decades and centuries (Crutzen and Andreae, 1990; Page et al., 2002; Tosca et al., 2013). It is hence necessary to explore fire characteristics with special considerations of their multi-scale variability and feedback.

From a global perspective, fires occur progressively more frequently towards the tropics (Mouillot and Field, 2005). Tropical savanna and forest burning contribute approximately 80% of global

open fire emissions (Bond et al., 2013). However, tropical regions also feature a great diversity of climate-weather systems that affect fire occurrence and seasonality. In the tropical Northern Hemisphere, fires over tropical southern Mexico and Central America (SMCA) occur during the Feb-May dry season and peak in April-May (Magi et al., 2012). These fire activities have a substantial influence on local air quality and human health (e.g., over Mexico City [19-20° N, 98-100°W] and the Yucatan region (Crounse et al., 2009; Yokelson et al., 2007; Yokelson et al., 2009). Fire emissions over the SMCA region also affect the eastern US after long-range transport (Kreidenweis et al., 2001; Lee et al., 2006; Rogers and Bowman, 2001). Understanding the processes that shape fire variabilities over this region is hence important locally (for air quality and fire management) and over broader regions.

Here, for the first time, we report a distinct quasi-biennial variability of fire activities over the southern Mexico and Central America region (SMCA, 10-25°N, 80-100°W) during the peak burning months (April – May) over 2003-2019 by validating different fire characteristics with the use of multiple independent datasets. We further explore the dominant causes of this quasi-biennial signal and provide concrete evidence for positive fire-precipitation feedback on short timescales to amplify the quasi-biennial signal based on model simulations.

2 Data and Methods

2.1 Observations

Two sets of fire emission inventories were used to investigate the interannual variability of fire activities. The Global Fire Emissions Database with small fires version 4.1 (GFED v4.1s) is a bottom-up inventory that generates fire-consumed dry matter using fire-burned areas combined with emission factors (Giglio et al., 2013; Randerson et al., 2012). GFED v4.1s provides monthly mean fire-consumed dry matter in total and for individual fire types at 0.25-degree spatial resolution. The Quick Fire Emissions Dataset (QFED) is a top-down emission inventory that generates fire emissions by using empirical relationships between fire-consumed dry matter and fire radiative power (Koster et al., 2015). Daily emissions of fire-emitted species at 0.1 horizontal resolution from QFED version 2.5 were examined. Since the interannual variations of different species are consistent, only variation of fire-emitted black carbon (BC) is shown here. We focused on the fire activities after 2003 to exclude the influence of the extremely strong ENSO events,

specifically the 1997/1998 El Niño event and the subsequent 1998-2000 La Niña event, which are among the most powerful ENSO events in recorded history.

We also examined the interannual variation of fire-induced changes in aerosol optical depth based on the MERRA-2 reanalysis data (Gelaro et al., 2017) and Level 3 version 4.2 CALIPSO satellite dataset (Winker et al., 2013). For the MERRA-2 data, monthly mean BC aerosol optical depth (AOD) was used for a better comparison with the BC emission from QFED emission data. The CALIPSO product divides aerosol into six sub-types, and the gridded monthly mean 532nm AOD for the biomass burning aerosol type under all-sky conditions was analyzed. We used the MODIS version 6.1 gross primary productivity (GPP) product (MOD17A2H, (Running, 2021)), which measures the growth of the terrestrial vegetation as a proxy for fuel load. A cumulative 8-day composite of GPP values is provided with a 500m pixel size. The average of GPP in the month (March) prior to the burning season is examined.

In order to investigate the climate influence on fire activities, we analyzed monthly mean temperature and maximum temperature from the Climatic Research Unit gridded Time Series (CRU TS) version 4.06 (Harris et al., 2014). The dataset is constructed based on station observations and provides monthly data over the global land surface at 0.5-degree resolution. Apart from the CRU dataset, two sets of satellite observations of precipitation were analyzed: the monthly Integrated Multi-satellitE Retrievals for GPM (IMERG) precipitation estimates at 0.1 degrees (Huffman et al., 2015) and the 1-degree daily (version 1.3), 2.5-degree monthly (version2.3) Global Precipitation Climatology Project (GPCP) precipitation estimates (Adler et al., 2018; Adler, 2017). IMERG is intended to intercalibrate and merge satellite microwave precipitation estimates together with microwave-calibrated infrared satellite estimates and precipitation gauge analyses (Huffman et al., 2020). Monthly mean 500hPa vertical velocity (ω) at 2.5 degrees from NCEP/NCAR reanalysis (Kanamitsu et al., 2002) and 10m wind speed at 0.25 degrees from ERA5 reanalysis (Hersbach et al., 2020) were also used in our work. In order to understand the interannual variation of precipitation, we examined the relationship between precipitation and ten different teleconnection patterns, including Atlantic Meridional Mode (AMM), East Pacific/North Pacific Oscillation (EP/NP), ENSO, North Atlantic Oscillation (NAO), North Tropical Atlantic index (NTA), Pacific North American index (PNA), Tropical Northern Atlantic index (TNA), Tropical Southern Atlantic index (TSA), Western Hemisphere

warming pool (WHWP), Quasi-biennial Oscillation (QBO). These indice and their detailed definitions can be obtained from https://psl.noaa.gov/data/climateindices/list/.

2.2 Model experiment

The CESM2.1.0 model with the Community Atmosphere Model version 6 (CAM6) (Danabasoglu et al., 2020) was used to investigate the feedback of fire-emitted aerosols on precipitation. The F2000 component set was used with the prescribed sea surface temperature in the year 2000. The horizontal resolution is set as 0.9-degree latitude by 1.25-degree longitude with 32 vertical levels. Two groups of simulations were conducted. Each was driven by the representative fire emissions in strong and weak fire years and referred to as Case_Strong and Case_Weak. The difference in variables (e.g., temperature and precipitation) between the two cases (Case_Strong minus Case_Weak) indicate the influence, or difference in feedback, caused by stronger fire emissions. As our work focused on the influence of fire activities over SMCA, only fire emissions over the SMCA region were considered. Since fire emissions and anthropogenic emissions are specified separately in the CESM2 model, we modified the default fire emission inventory (Van Marle et al., 2017) in CESM2.1.0 accordingly while global anthropogenic emissions were kept unchanged and remained the same between cases. Given that composite analysis indicates fire emissions in weak fire years are approximately half those in strong fire years. We simply used the average of fire emissions during strong fire years in Case_Strong, and reduced these by half in Case_Weak. More subtle changes in fire locations between strong and weak fire years are hence ignored. Furthermore, global climate models have long been found to underestimate fire-induced changes in aerosols (Zhong et al., 2022). Hence, in order to ensure the simulated difference in fire-induced AOD between Case_Strong and Case_Weak is comparable to observations, the default inventory is multiplied by a factor of 3 to ensure the simulated fire-induced AOD changes are comparable to observations. For each group, 9 ensemble simulations were performed with slight differences in their initial conditions. The ensemble mean is calculated as the average of 9 members. All simulations start on Jan.1 with a 3-month spin-up time. The T-test is used to identify statistically significant differences between Case_Strong and Case_Weak.

3 Results

3.1 Biennial variability of fire activities

We focus on the southern Mexico and Central America region (SMCA) covering both the Yucatan region and Mexico City. Major fire types in this region consist of deforestation fires, savanna fires, and agricultural waste burning, which respectively are estimated to consume 45.5%, 42.1%, and 12.40% of the total burned dry matter during the peak burning months (Apr-May) of the 17-year (2003-2019) study period.

As shown in Fig. 1a, GFEDv4.1s estimates of the regional sum of the total dry matter consumed by fire activities feature obvious quasi-biennial variability. Generally speaking, fire activities in odd-numbered years show higher consumption of dry matter than adjacent even-numbered years with the only exception of the year 2016, which might be related to a long-lasting El Niño event spanning 2014-2016. Composites of fire consumption of dry matter indicate enhanced fire activities along both sides of the high terrains in odd-numbered years, and the most profound difference appears over the bordering area between southern Mexico and Guatemala (Fig. S2). The average fire-consumed dry matter here differs by more than a factor of 6 between odd-numbered and even-numbered years.

The quasi-biennial variability of fire activities is also evident when examining fire emissions of typical fire-emitted species based on the QFED inventory (Fig. 1b). Similarly, fire-emitted BC in odd-numbered years is higher than those in the adjacent even-numbered years, when considering both regional mean and medium values. Furthermore, among the 9 odd-numbered years, fire activities in years 2003/2011/2013 show the highest three BC emission, which is also consistent with results from the GFEDv4.1s dataset. Hence, the two independent fire emission inventories agree on the interannual variation of fire activities.

Apart from cross-checking different fire emission inventories, we further validated the variability of fire activities by investigating fire-induced changes in AOD (Fig. 1c). BC AOD from MERRA-2 reanalysis and AOD of biomass burning aerosol type from CALIPSO were adopted to represent fire activities. Basically, the interannual variation of fire-related AOD in both datasets agrees well with the estimates from fire inventories, thus providing additional support for the quasi-biennial variability of fire activities in the peak burning months over SMCA. Overall, the intercomparison between multiple datasets indicates a consistent quasi-biennial variability in different fire

characteristics, including fire-consumed dry matter, fire-emitted aerosols as well as fire-related changes in optical properties. Note that among the four datasets, the GFEDv4.1s inventory and MERRA-2 reanalysis data provide data till the year of 2023, and the quasi-biennial variability in the extended time series remains robust till 2023 (Fig. S1). To describe this quasi-biennial variability for convenience, we hereafter refer to the odd-numbered (even-numbered) years that have higher (lower) fire consumptions of dry matter than adjacent years as strong (weak) fire years.

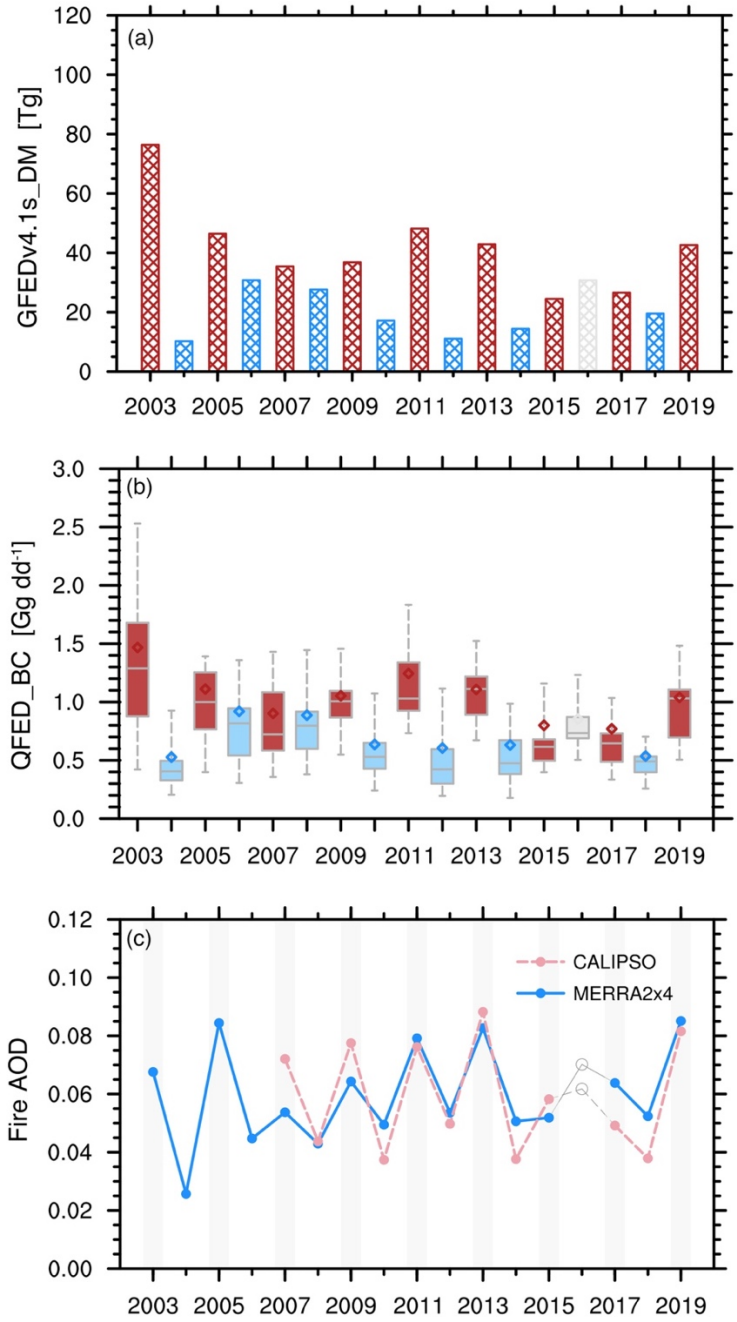

Figure 1. Interannual variations of different fire characteristics during the peak burning season (Apr-May) over Southern Mexico and Central America (SMCA). (a) Regional sum of the total dry matter consumed by fire activities based on the GFEDv4.1s emission data. (b) Distributions of the daily sum of fire-emitted black carbon (BC) over SMCA based on QFED emission data. Boxes denote the 25th and 75th percentiles. Bars outside the boxes denote the 10th and 90th percentiles. Bars within the boxes denote the medium values, and dots denote regional mean values (c) Regional mean aerosol optical depth (AOD) of smoke aerosols from CALIPSO product and BC AOD from MERRA-2 reanalysis. The odd-numbered years with strong fires are denoted by the grey bars.

3.2 Dominant role of the biennial variability of precipitation

Fire activity is strongly affected by factors including fire ignition, fuel load, and climate-weather conditions (Flannigan et al., 2005; Archibald, 2016; Ichoku et al., 2016; Veira et al., 2016). Fire ignition is affected by both natural lightning and human activities (Pechony and Shindell, 2009). Since there is no policy to regulate fire activities with periodicity, it is unlikely that human impact is the major driving force. Fuel availability may play a role in the interannual variation of fires. After having examined the GPP (surrogate for fuel load) prior to the burning season, we found little evidence regarding the role of fuel availability in contributing to the interannual variation of fires (Fig. S3). Lower values of GPP are found in some strong fire years compared to their adjacent years, e.g., the years 2003 and 2005. Correlations between regional GPP and fire-consumed dry matter are even slightly negative.

Close yet complex relationships between ambient conditions (e.g., humidity, temperature, precipitation) and fire activities have been widely revealed in previous studies (Cary et al., 2006; Gillett et al., 2004; Prasad et al., 2008). For example, warm temperatures could increase fire activity by increasing evapotranspiration and also by lengthening fire duration, while both the timing and amount of precipitation could regulate fire behavior. To identify the climatic factors that might be responsible for the quasi-biennial variation of fire activities, we first examined the relationships between fire-consumed dry matterand different meteorological variables (Table 1). Temporal correlations of their regional mean values indicate that fire activities are enhanced with warmer mean and maximum temperature (R=0.47 and 0.59), but are weakened with higher precipitation (R=-0.69). Though wind speed could affect the spread of fire activities, the insignificant correlation signifies a minor influence on the interannual scale (Fig. S3). Other meteorological metrics such as vapor pressure deficit (VPD) and relative humidity (RH) are also frequently used to help understand fire-meteorology interactions. Here we found the interannual variations of regional mean VPD and RH are highly correlated with precipitation (R =-0.8 for VPD and R=0.7 for RH, respectively) and temperature (R = 0.7 for VPD and R = -0.5 for RH, respectively) over the SMCA region.

Figure 2 shows the spatial distribution of correlations of fire-consumed dry matter with precipitation and mean temperature during peak burning months. With respect to precipitation, negative correlations cover almost the entire SMCA region and are statistically significant over major fire source areas from Yucatan extending southwestward to Chiapas. In contrast, positive

correlations between fire-consumed dry matter and maximum temperature mainly appear over the northern part of SMCA (southern Mexico), albeit with less influence over Central America (e.g., fire source areas in Guatemala). Hence, the interannual variability of precipitation affects the variation of fire activities on a wider spatial range. We next examined closely the time series of regional mean precipitation and temperature (Fig 3). Here regional mean values are calculated using data over land so that only climate conditions that could directly affect fire activities are considered. Two independent precipitation datasets show similar temporal evolution patterns. An obvious quasi-biennial variability is seen in regional mean precipitation. More suppressed precipitation (compared to adjacent years) corresponds well to the strong fire years (excluding the year 2016). Furthermore, spectral analysis confirms a statistically significant periodicity of approximately 2 years (0.042 cycles per month) for precipitation, suggesting the mediation of precipitation on the quasi-biennial feature of fire activities. Meanwhile, the quasi-biennial signal is less apparent in mean and maximum temperatures. For instance, temperatures in the strong fire years 2007 and 2009 are smaller in magnitude compared to adjacent weak fire years. Nevertheless, higher mean and maximum temperatures (compared to adjacent years) appear in 2003 and 2011, which combines with the suppressed precipitation, contributing to the abnormally high fire-consumed dry matter in the two years. As a result, while both temperature and precipitation are critical in shaping fire activities over the SMCA region, precipitation plays a more fundamental role in formulating the quasi-biennial variability of fires.

Table 1. Correlations between the regional sum of fire consumed dry matter based on the GFEDv4.1 data and regional mean values of different meteorological variables (including the monthly mean precipitation from IMERG dataset, mean temperature, maximum temperature from CRU dataset, and 10m wind speed from ERA5 reanalysis) averaged in the peak fire season (April-May).

Correlation	Precipitation	Mean Temperature	Maximum Temperature	10m wind speed
Fire-consumed Dry matter	-0.69*	0.47*	0.59*	0.29

* represents the correlations are statistically significant at the 90% confidence level based on the student's T-test.

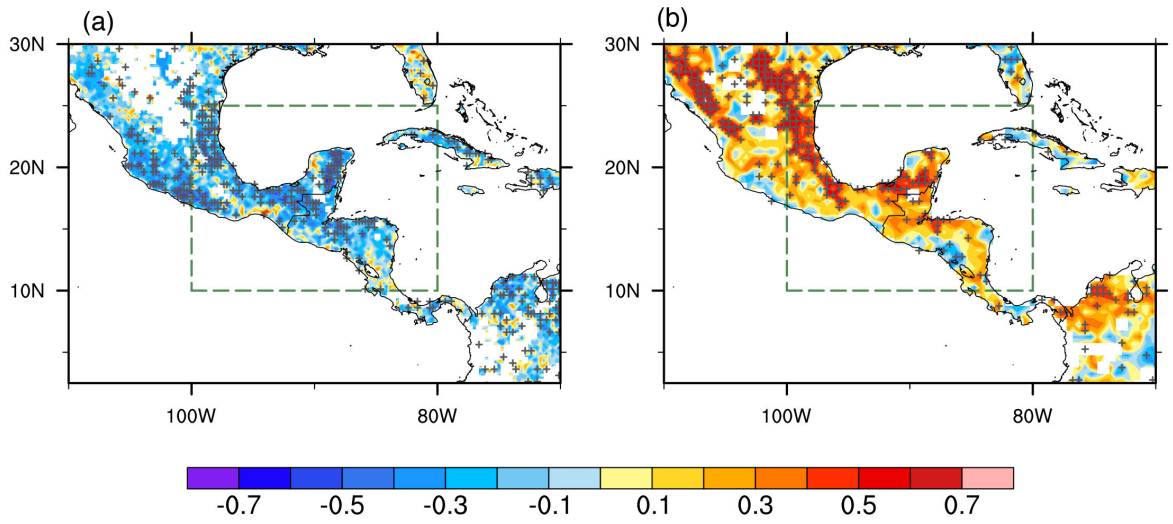

Figure 2. The influence of meteorological factors on fire activities over SMCA. Spatial distributions of grid-to-grid correlations between fire-consumed dry matter and (a) precipitation from IMERG and (b) maximum temperature from CRU during the peak fire season (Apr-May) over 2003-2019. Stippling indicates the correlations are statistically significant at the 90% confidence level based on the student's T-test. The green boxes denote the SMCA region.

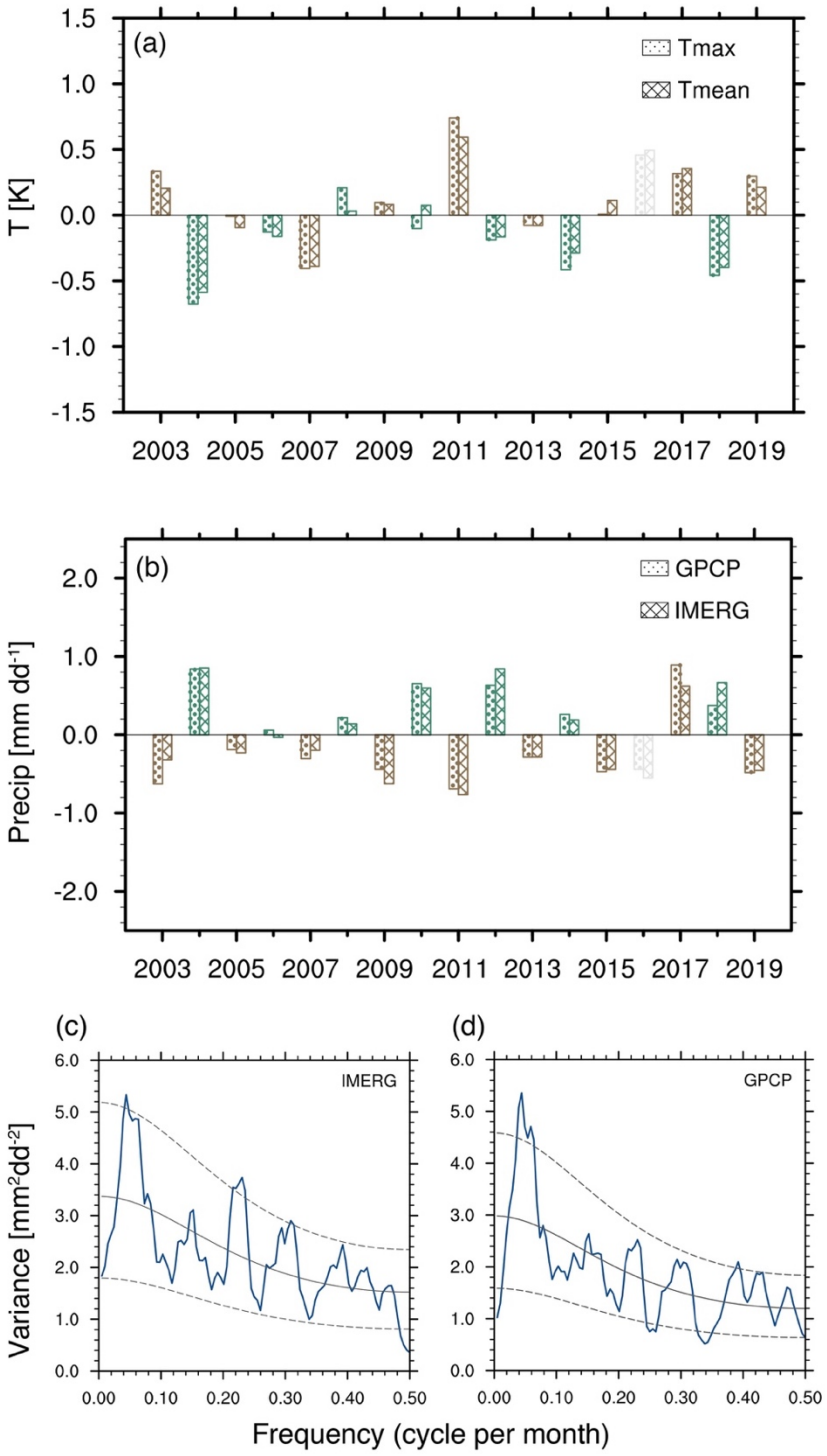

Figure 3. Interannual variability of meteorological factors in peak fire season over SMCA. Time series of the Apr-May (a) mean/maximum temperature and (b) mean precipitation anomalies (with respect to the 2003-2019 climatology mean) averaged over SMCA (land only). (c) Spectral analysis of monthly mean precipitation averaged over SMCA during 2003-2019. The black solid line and dashed lines represent the red noise curve and the 10%, 90% confidence interval.

The leading role of precipitation on the interannually varying fire activities is evident in the composite analysis, as shown by the contrast of reduced precipitation in strong fire years and enhanced precipitation in weak fire years (Fig. 4a). The composite analysis further shows that the anomalous precipitation is closely related to vertical motions, with stronger subsidence corresponding to weaker precipitation (Fig. 4b). It is worth noting that to the northwest of the SMCA region near the southeast US, composited precipitation and vertical velocity also differ significantly between strong and weak fire years albeit of opposite signs. Consistent changing features of precipitation and vertical velocity are also captured when regressing the two variables on the regional mean precipitation over SMCA (Fig. 4c-d). The negative regression coefficients indicate a stronger upward (downward) motion corresponding to higher (weaker) precipitation. In sum, for a specific year, stronger subsidence and the subsequent suppression of precipitation tend to amplify fire activity in that year, and vice versa for the year with weakened subsidence and less suppression effect of precipitation. In this way, the quasi-biennial variability of precipitation leads to the same interannual variability of fire activities.

Precipitation patterns over the SMCA region and the variability are associated with complex physical forcing mechanisms, e.g. changes in sea surface temperature, low-level winds, the strength and position of ITCZ et al., and all of these processes could be modulated by large-scale modes of atmospheric and oceanic variability (Duran-Quesada et al., 2017; Perdigon-Morales et al., 2019; Amador et al., 2006). Here we chose 10 typical teleconnection patterns, for example, the El Niño-Southern Oscillation, (ENSO), based on previous studies and examined their relationships with SMCA precipitation in the peak fire months. After calculating the correlations between Apr-May mean precipitation and the index in varying months (both simultaneously and previous to the fire season), we found that the precipitation in the fire season is mostly affected by the East Pacific/North Pacific Oscillation (EP/NP) pattern in the previous two months (Feb-Mar). Generally, the positive phase of EP/NP features negative height anomalies and an enhanced cyclonic circulation over the eastern United States (Athanasiadis et al., 2010). Consequently, in the following fire season, this causes anomalous upward and downward motions over the southeastern US and the SMCA region respectively (Fig. S4), and enhances precipitation over the southeastern US yet suppressing precipitation over the SMCA region (Fig. 5). Hence, the EP/NP teleconnection results in an opposite responding pattern in precipitation and vertical velocity

between the eastern US and the SMCA region. This further explains the similar contrasting spatial pattern that is found in the aforementioned composite and regression analysis.

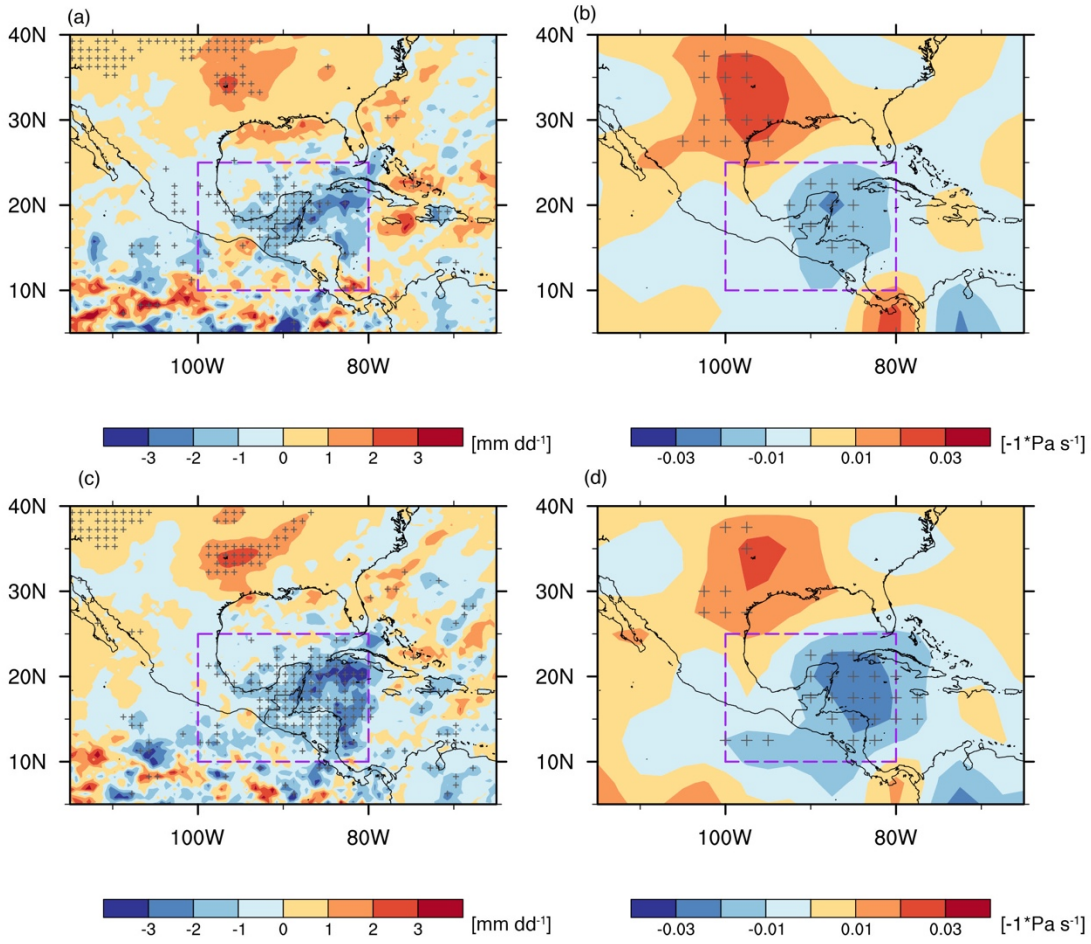

Figure 4. Varying characteristics of precipitation and circulations. Differences of composites of (a) precipitation and (b) 500hPa vertical pressure velocity (reversed signs) between strong and weak fire years. Stippling indicates the differences are statistically significant at the 90% confidence level based on T-test. Regressions of Apr-May mean (c) precipitation and (d) 500hPa vertical velocity on the regional mean precipitation over SMCA (reversed signs) during 2003-2019. Stippling indicates regression coefficients are statistically significant at the 90% confidence level based on the T-test.

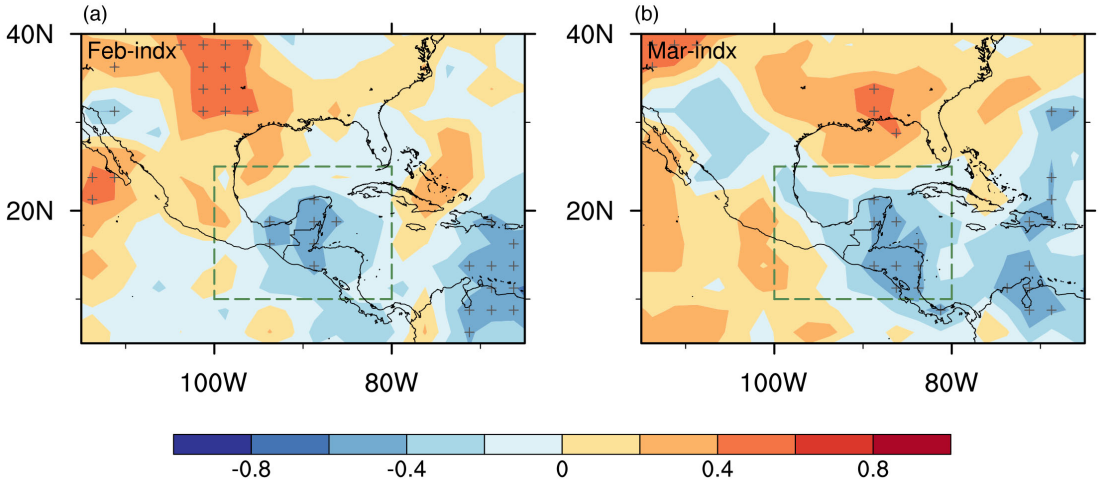

Figure 5. Influence of the EP/NP teleconnection pattern on precipitation in peak fire season. Spatial distributions of correlations of EP/NP index in (a) February and (b) March with the mean precipitation in the peak fire season (Apr-May) during 2003-2019. Stippling indicates the correlations are statistically significant based on the student's T-test.

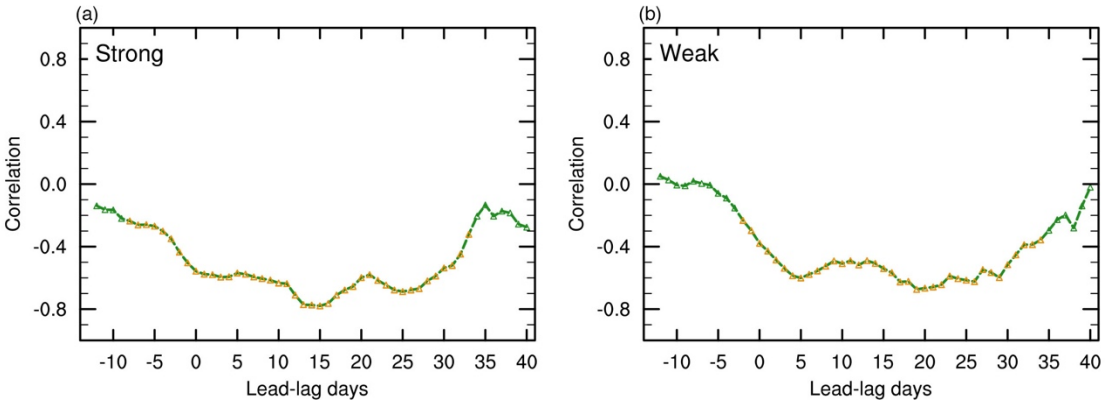

Figure 6. Different duration of fire-precipitation interaction. Lead-lag correlations between regional mean daily precipitation and fire emission composites in (a) strong fire years and (b) weak fire years over SMCA. Positive lead-lag days represent that precipitation leads while negative lead-lag days represent fire emissions leads. Correlations that are statistically significant at the 90% confidence level based on Student's t-test are marked with yellow triangles.

3.3 Positive feedback between enhanced fire emissions and suppressed precipitation

Previous studies have found that fire-emitted aerosols could interact with synoptic weather, which in turn affects fire variability (Huang et al., 2023). In view of this, one concern is if fire and precipitation interact on short timescales (i.e., within individual fire seasons) in our case over the SMCA region, and if so, how this feedback modulates the quasi-biennial variability of precipitation and fire activities. We first calculated lead-lag correlations between daily precipitation and fire emissions to identify the short-term fire-precipitation interaction. As shown in Fig. 6 lead-lag correlations between regional mean precipitation and fire emission are generally similar whether fire activities in strong or weak fire years are considered. When precipitation leads, precipitation negatively correlates with fire emission for more than 20 days, signifying a long-lasting suppression effect of precipitation on fire activities. In other words, weakened precipitation would enhance fire activities. Meanwhile, when fire leads, negative correlations indicate that increased fire activities would further suppress precipitation at shorter timescales (3-5 days) through rapid adjustments. In short, there is a two-way interaction between precipitation and fire activities on short timescales with different duration, forming a positive feedback loop.

We also conducted sensitivity simulations to investigate the underlying processes involved in the fire-precipitation feedback. Fig. 7 shows the simulated difference in AOD (referred to as fire AOD) between Case_Strong and Case_Weak. Both the spatial pattern and magnitude agree well with the difference in AOD between strong and weak fire years based on CALIPSO observations. Compared to the spatial patterns of fire consumption in Fig. 7, we can clearly see two transport pathways of fire-emitted aerosols due to the continental divide by the Central Mexican Plateau. North of 15°N, fire-emitted aerosols are transported northward by the subtropical high, among which large amounts accumulate over the downstream Gulf of Mexico due to the block of the high terrain, and the rest is further transported northward reaching the southeastern US; South of 15°N, prevailing easterlies transport fire-emitted aerosols directly westward, far away to the eastern Pacific.

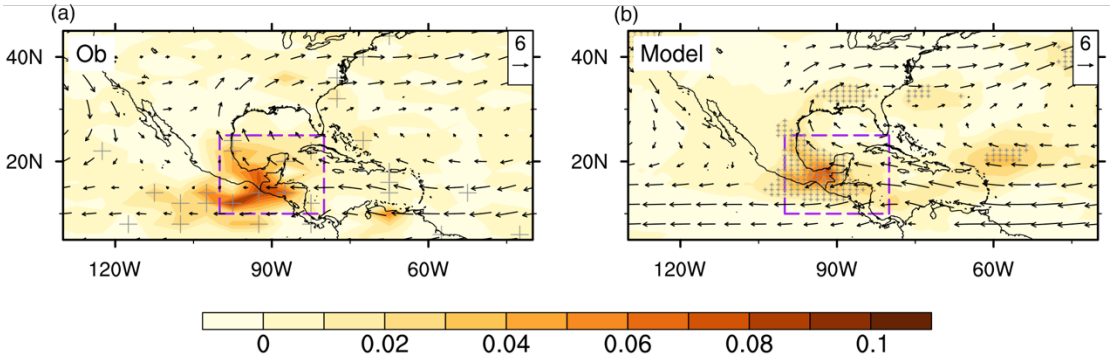

Figure 7. Evaluation of model simulated fire-induced AOD. (a) Spatial distributions of differences in biomass burning AOD between strong and weak fire years from CALIPSO satellite data. (b) Differences in simulated AOD between Case_Strong and Case_Weak. Mean 850hPa wind vectors from (a) NCEP reanalysis data averaged in all years and (b) model simulations averaged between both cases are overlaid respectively. Stippling indicates the differences in AOD are statistically significant based on T-test.

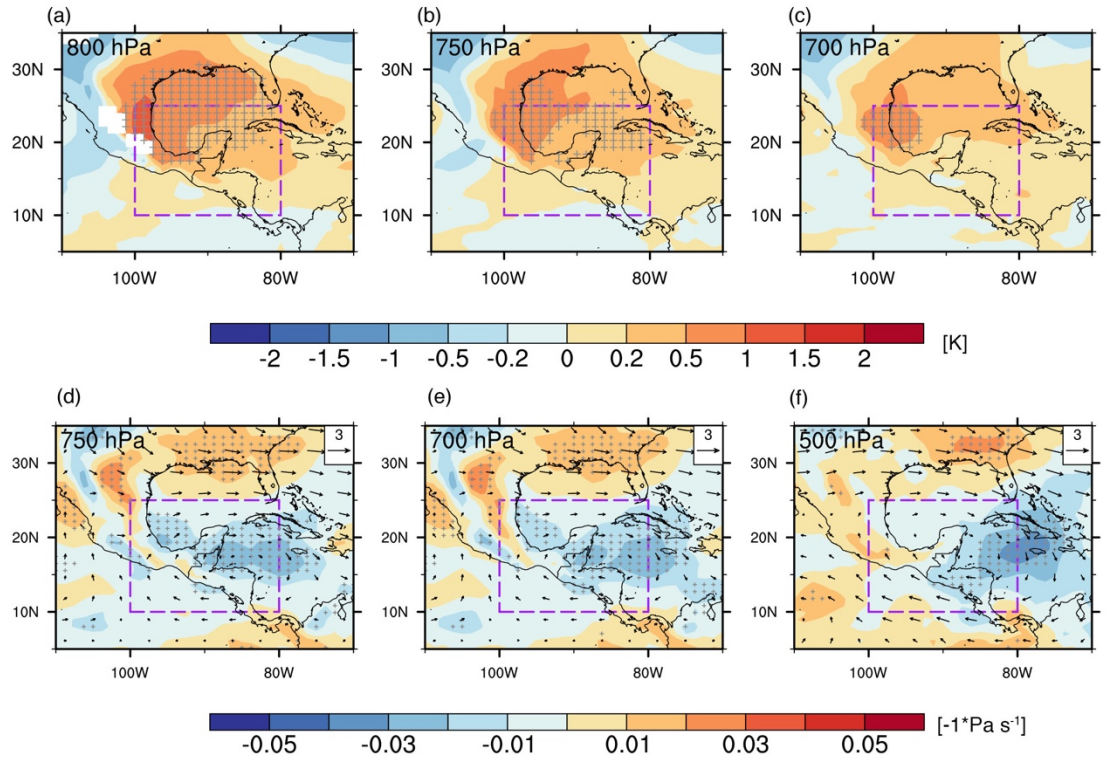

Figure 8. Changes in meteorological variables induced by fire-emitted aerosols. Differences in (a-c) atmospheric temperature and (d-f) vertical pressure velocity (reversed signs and shaded colors) at different vertical levels between Case_Strong and Case_Weak. Changes in horizontal winds between the two cases are overlaid in (d-f). Stippling indicates the differences are statistically significant at the 90% confidence level based on T-test.

Considering the northward pathway, with the stack of light-absorbing BC aerosols, air temperature warms up by approximately 1-2K, and this warming extends from 800hPa to 700hPa where BC aerosols suspend (Fig. 8a-c). Vertical slices of the temperature anomalies indicate significant warming to the north (downstream) of the fire source regions (Fig. 9a). In response to this warming, the air above the fire aerosol layers rises up (Fig. 8d-f). The anomalous ascending motion covers from the Gulf of Mexico to the southeastern US, with the maximum center located near the Gulf of Mexico. This abnormal ascending motion, on one hand, enhances precipitation downstream of the fire source regions, and on the other hand forces a compensating anomalous descending motion over the SMCA region and suppresses the precipitation over the fire source regions (Fig. 9b-c). This simulated opposite change in precipitation resembles the spatial pattern of the composited precipitation difference between strong and weak fire years (Fig. 4a), suggesting that fire-precipitation interaction reinforces the contrast of precipitation between strong and weak fire years. Therefore, the model simulations confirm a positive fire-precipitation feedback loop on the short timescale within the fire season.

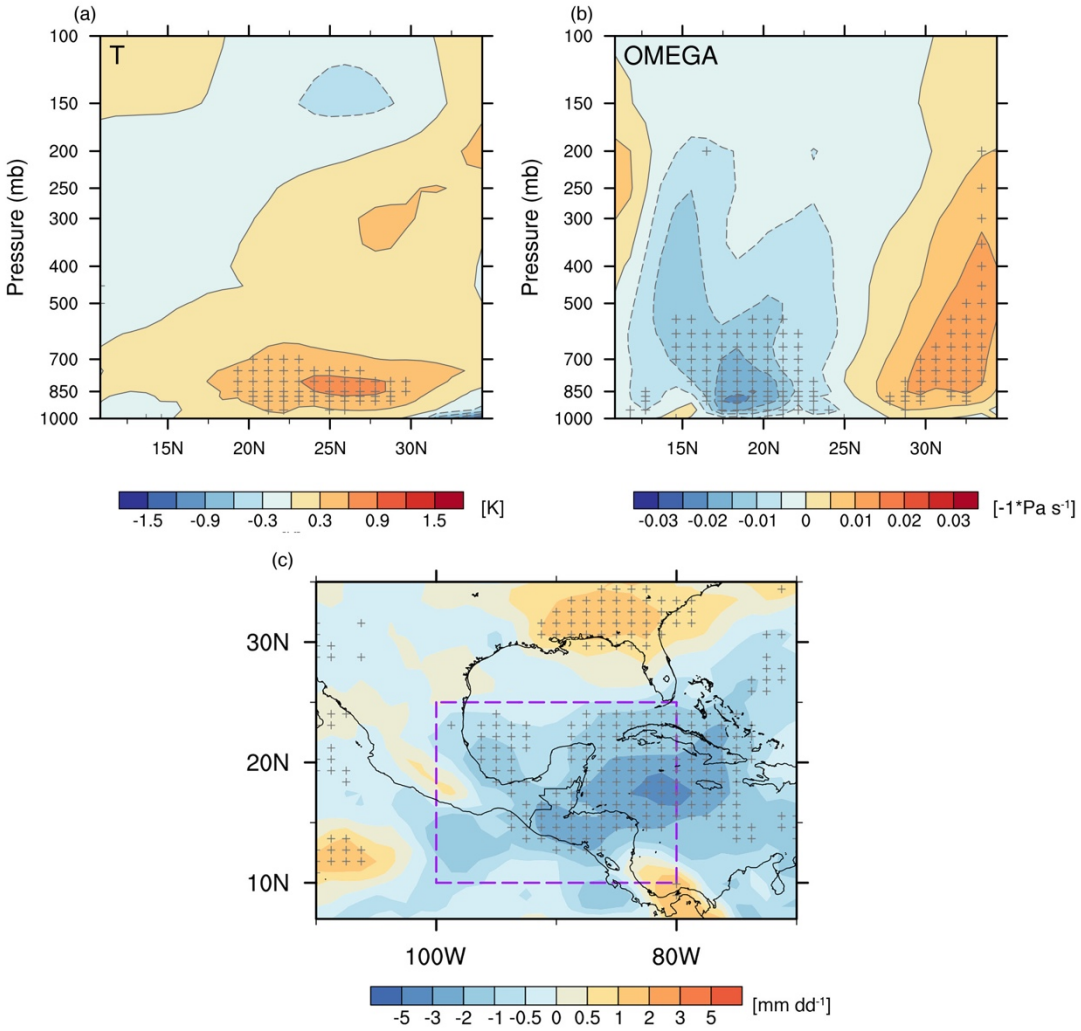

Figure 9. Vertical slices of differences in (a) atmospheric temperature and (b) pressure velocity averaged along [80 ° -100 ° W] between Case_Strong and Case_Weak. (c) Differences in precipitation between Case_Strong and Case_Weak. Stippling indicates the differences are statistically significant based on T-test.

As illustrated in Fig. 10, originally on the interannual scale, fire activities over the SMCA region exhibit a significant quasi-biennial variability that is predominantly determined by the quasi-biennial variation of precipitation. On this basis, there is an additional two-way interaction between fire and precipitation on short timescales. Typically, precipitation suppresses fire activities with a time lag of more than 20 days, while fire-emitted aerosols suppress precipitation by modifying circulations with a timescale of 3-5 days. That is to say, for a year with abnormally weak precipitation, fire activities would get amplified, which in turn further weakens precipitation. In

this way, the short-term positive feedback loop ultimately enhances the quai-biennial variability of precipitation and fire activities over the SMCA region.

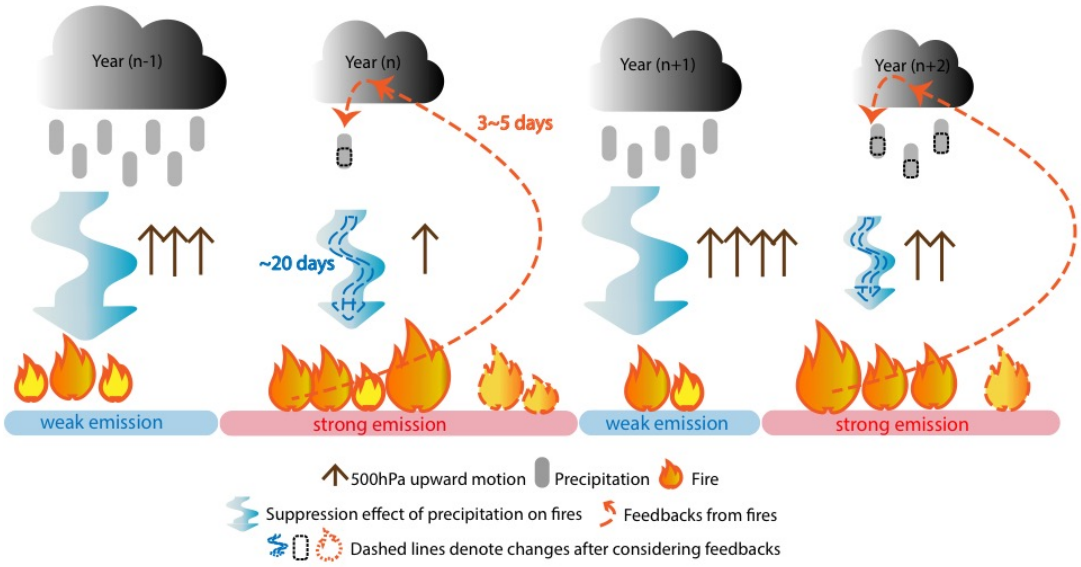

Figure 10. A schematic diagram illustrating how multi-scale fire-precipitation interactions shape the quasi-biennial variability of fires over SMCA. On the interannual scale, the quasi-biennially varying precipitation triggers a similar quasi-biennial variability of fire activities via its suppression effect. Compared to adjacent years, a weaker precipitation year will facilitate stronger fires. On short timescales within each fire season, there is a positive feedback loop between fire and precipitation (denoted by dashed lines). The suppression effect of precipitation lasts long for approximately 20 days, while fires affect precipitation through a rapid adjustment of 3-5 days. In the weaker precipitation year, stronger fire activities emit more aerosols, which by mediating temperature and circulations, ultimately suppress precipitation over the fire source region. Such short-term interactions between precipitation and fire amplify the magnitude of anomalous fire and precipitation in individual years and enhance the quasi-biennial variability of both precipitation and fire.

4 Conclusion and Discussion

Fires play an important role in the Earth system, and the complex interaction between fire activities and ambient conditions poses a great challenge to fire prediction and management. This study identifies a distinct quasi-biennial variability of fire activities over the SMCA region during 2003-2019 on the basis of different fire metrics. Both the bottom-up (GFEDv4.1s) and top-down(QFED) emission inventories show relatively higher fire consumption (or emission) in the odd-numbered years than the adjacent even-numbered years with the only exception of the year 2016. Moreover, fire-induced changes in AOD also reveal consistent quasi-biennial variation.

By examing the relationships between fire consumption and different meteorological variables, our analysis indicates that the quasi-biennial signal is dominated by the quasi-biennially varying precipitation, while the influence of temperature is mostly reflected in a few extremely strong fire years. Typically, strong fire years correspond to suppressed upward motions and weakened precipitation. The quasi-biennial variability of precipitation is seen in the time series of the regional mean precipitation over SMCA and the spectral analysis, and is closely related to the EP-NP teleconnection pattern in the two months previous to the fire season. The positive phase of the EP-NP pattern implies enhanced precipitation over the southeastern US (downstream of the SMCA), albeit reduced precipitation over the SMCA region.

On the other hand, we further found that positive feedback exists between fire-emitted aerosols and precipitation on short timescales and acts to amplify the quasi-biennial oscillations in both fire and precipitation over the SMCA region. Lead-lag correlations between daily fire emission and precipitation suggest that the two-way interactions occur with different duration. The suppression effect of precipitation lasts for approximately 20 days, while fire-emitted aerosols weaken precipitation through rapid adjustments of 3-5 days. Furthermore, model simulations reveal that compared to weak fire years, more fire-emitted aerosols are transported downstream and accumulate near the Gulf of Mexico in strong fire years. These suspended light-absorbing BC aerosols warm the low-level atmosphere by 1-2K and induce anomalous ascending motion aloft 700hPa. A compensating descending motion is subsequently forced over the SMCA region, which ultimately suppresses the precipitation over the fire source region and hence forms a positive feedback loop.

These findings provide useful information relevant to the fire control and mitigation of air quality over the SMCA region. Given that fire activities over the SMCA represent a typical tropical fire regime, our work may also provide new insight into some fundamental features of fires in the Earth System. The mechanism may also operate elsewhere useful on the planet. While precipitation is demonstrated to play the primary role in determining the periodicity of fire activities over the SMCA region, the fundamental cause of the quasi-biennial variability of precipitation is unknown. Currently, we have only shown that the EP-NP teleconnection, among all selected indexes, exerts the most influence on the interannual variability of precipitation. Other teleconnection patterns, e.g., ENSO, despite their insignificant correlations with SMCA precipitation, may affect the circulation and precipitation over the southeastern US or over the neighboring Intra-American Sea (Anthony Chen and Taylor, 2002), and hence might more or less affect the precipitation over the SMCA region. Moreover, though we demonstrated positive feedback between fire-emitted aerosols and precipitation exists on short timescales, to what extent this feedback contributes to the quasi-biennial variability of fire activities remains unquantified due to the absence of coupled fire-climate interactions in current model simulations. Future efforts to quantify how different factors and feedback work together to shape the quasi-biennial variability of precipitation and fire activities using interactive fire-climate models would further benefit the prediction and management of fire activities over the SMCA region.

Data availability

The GFED v4.1s fire emission data is available at http://www.globalfiredata.org/data.html. The CRU TS v.4.06 can be found at https://crudata.uea.ac.uk/cru/data/hrg/. The QFEDv2.5 data can be found at http://ftp.as.harvard.edu/gcgrid/data/ExtData/HEMCO/QFED/v2018-07/. The MODIS GPP data is available from https://lpdaac.usgs.gov/products/mod17a2hv061/The MERRA-2 reanalysis data can be found at https://gmao.gsfc.nasa.gov/reanalysis/MERRA-2/data_access/. The IMERG precipitation dataset can be obtained from https://gpm.nasa.gov/data/imerg. The GPCP dataset can be obtained from https://www.ncei.noaa.gov/products/climate-data-records/precipitation-gpcp-daily. Teleconnection indices can be found at https://psl.noaa.gov/data/climateindices/list/. The NCEP-NCAR reanalysis is obtained from https://www.esrl.noaa.gov/psd/data/gridded/data.ncep.reanalysis2.html. The CALIPSO product is available at https://asdc.larc.nasa.gov/project/CALIPSO/CAL_LID_L3_Tropospheric_APro_AllSky-Standard-V4-20_V4-20.

Author contribution

Y.L. and Y. Q. conceived of the presented idea. Y. Q., Y. W. and Y. L. developed the theory. Y. L. performed the computations and verified the methods. Y. Q., Y. L. and K. Z wrote the first draft of the manuscript. All authors contributed to the interpretation of the results and writing/revision of the final manuscript.

Competing interests

Yun Qian and Hailong Wang are members of the editorial board of Atmospheric Chemistry and Physics. The authors have no other competing interests to declare.

Acknowledgments

We benefited from discussing some aspects of this work with John M Wallace and Dae-Hyun Kim. Yawen Liu is supported by the National Natural Science Foundation of China (No. 42325506). This study is also supported by the U.S. Department of Energy's Office of Science as part of the Regional and Global Modeling and Analysis program. The Pacific Northwest National Laboratory is operated for DOE by Battelle Memorial Institute under contract DE-AC05-76RL01830. We are grateful to the High-Performance Computing (HPC) and the Massive Data Center (MDC) at Nanjing University for the numerical calculations.

References

Abram, N. J., Henley, B. J., Sen Gupta, A., Lippmann, T. J. R., Clarke, H., Dowdy, A. J., Sharples, J. J., Nolan, R. H., Zhang, T. R., Wooster, M. J., Wurtzel, J. B., Meissner, K. J., Pitman, A. J., Ukkola, A. M., Murphy, B. P., Tapper, N. J., and Boer, M. M.: Connections of climate change and variability to large and extreme forest fires in southeast Australia, Commun Earth Environ, 2, ARTN 810.1038/s43247-020-00065-8, 2021.

Adler, R. F., Sapiano, M. R. P., Huffman, G. J., Wang, J. J., Gu, G. J., Bolvin, D., Chiu, L., Schneider, U., Becker, A., Nelkin, E., Xie, P. P., Ferraro, R., and Shin, D. B.: The Global Precipitation Climatology Project (GPCP) Monthly Analysis (New Version 2.3) and a Review of 2017 Global Precipitation, Atmosphere, 9, ARTN 1310.3390/atmos9040138, 2018.

Adler, R. W., Jian-Jian; Sapiano, Mathew; Huffman, George; Bolvin, David; Nelkin, Eric; and NOAA CDR Program: Global Precipitation Climatology Project (GPCP) Climate Data Record (CDR), Version 1.3 (Daily), NOAA National Centers for Environmental Information. doi:10.7289/V5RX998Z, 2017.

Aguilera, R., Corringham, T., Gershunov, A., and Benmarhnia, T.: Wildfire smoke impacts respiratory health more than fine particles from other sources: observational evidence from Southern California, Nature Communications, 12, ARTN 149310.1038/s41467-021-21708-0, 2021.

Amador, J. A., Alfaro, E. J., Lizano, O. G., and Magana, V. O.: Atmospheric forcing of the eastern tropical Pacific: A review, Prog Oceanogr, 69, 101-142, 10.1016/j.pocean.2006.03.007, 2006.

Anthony Chen, A. and Taylor, M. A.: Investigating the link between early season Caribbean rainfall and the El Niño + 1 year, International Journal of Climatology, 22, 87-106, 10.1002/joc.711, 2002.

Archibald, S.: Managing the human component of fire regimes: lessons from Africa, Philosophical Transactions of the Royal Society B: Biological Sciences, 371, 20150346, 2016.

Athanasiadis, P. J., Wallace, J. M., and Wettstein, J. J.: Patterns of Wintertime Jet Stream Variability and Their Relation to the Storm Tracks, J Atmos Sci, 67, 1361-1381, 10.1175/2009jas3270.1, 2010.

Bond, T. C., Doherty, S. J., Fahey, D., Forster, P., Berntsen, T., DeAngelo, B., Flanner, M., Ghan, S., Kärcher, B., and Koch, D.: Bounding the role of black carbon in the climate system: A scientific assessment, Journal of Geophysical Research: Atmospheres, 118, 5380-5552, 2013.

Bowman, D. M., Balch, J. K., Artaxo, P., Bond, W. J., Carlson, J. M., Cochrane, M. A., D'Antonio, C. M., DeFries, R. S., Doyle, J. C., and Harrison, S. P.: Fire in the Earth system, science, 324, 481-484, 2009.

Bowman, D. M. J. S., Williamson, G. J., Abatzoglou, J. T., Kolden, C. A., Cochrane, M. A., and Smith, A. M. S.: Human exposure and sensitivity to globally extreme wildfire events, Nat Ecol Evol, 1, ARTN 005810.1038/s41559-016-0058, 2017.

Cary, G. J., Keane, R. E., Gardner, R. H., Lavorel, S., Flannigan, M. D., Davies, I. D., Li, C., Lenihan, J. M., Rupp, T. S., and Mouillot, F.: Comparison of the sensitivity of landscape-fire-succession models to variation in terrain, fuel pattern, climate and weather, Landscape ecology, 21, 121-137, 2006.

Crounse, J., DeCarlo, P., Blake, D. R., Emmons, L., Campos, T., Apel, E., Clarke, A., Weinheimer, A., McCabe, D., and Yokelson, R. J.: Biomass burning and urban air pollution over the Central Mexican Plateau, Atmospheric Chemistry and Physics, 9, 4929-4944, 2009.

Crutzen, P. J. and Andreae, M. O.: Biomass Burning in the Tropics - Impact on Atmospheric Chemistry and Biogeochemical Cycles, Science, 250, 1669-1678, DOI 10.1126/science.250.4988.1669, 1990.

Danabasoglu, G., Lamarque, J. F., Bacmeister, J., Bailey, D. A., DuVivier, A. K., Edwards, J., Emmons, L. K., Fasullo, J., Garcia, R., Gettelman, A., Hannay, C., Holland, M. M., Large, W. G., Lauritzen, P. H., Lawrence, D. M., Lenaerts, J. T. M., Lindsay, K., Lipscomb, W. H., Mills, M. J., Neale, R., Oleson, K. W., Otto-Bliesner, B., Phillips, A. S., Sacks, W., Tilmes, S., van Kampenhout, L., Vertenstein, M., Bertini, A.,

552 Dennis, J., Deser, C., Fischer, C., Fox-Kemper, B., Kay, J. E., Kinnison, D., Kushner, P. J., Larson, V. E.,
553 Long, M. C., Mickelson, S., Moore, J. K., Nienhouse, E., Polvani, L., Rasch, P. J., and Strand, W. G.: The
554 Community Earth System Model Version 2 (CESM2), J Adv Model Earth Sy, 12, ARTN
555 e2019MS00191610.1029/2019MS001916, 2020.

556 Ding, K., Huang, X., Ding, A. J., Wang, M. H., Su, H., Kerminen, V. M., Petaja, T., Tan, Z. M., Wang, Z.
557 L., Zhou, D. R., Sun, J. N., Liao, H., Wang, H. J., Carslaw, K., Wood, R., Zuidema, P., Rosenfeld, D.,
558 Kulmala, M., Fu, C. B., Poschl, U., Cheng, Y. F., and Andreae, M. O.: Aerosol-boundary-layer-monsoon
559 interactions amplify semi-direct effect of biomass smoke on low cloud formation in Southeast Asia, Nature
560 Communications, 12, ARTN 641610.1038/s41467-021-26728-4, 2021.

561 Duran-Quesada, A. M., Gimeno, L., and Amador, J.: Role of moisture transport for Central American
562 precipitation, Earth Syst Dynam, 8, 147-161, 10.5194/esd-8-147-2017, 2017.

563 Fang, K. Y., Yao, Q. C., Guo, Z. T., Zheng, B., Du, J. H., Qi, F. Z., Yan, P., Li, J., Ou, T. H., Liu, J., He,
564 M. S., and Trouet, V.: ENSO modulates wildfire activity in China, Nature Communications, 12, ARTN
565 176410.1038/s41467-021-21988-6, 2021.

566 Fasullo, J. T., Rosenbloom, N., and Buchholz, R.: A multiyear tropical Pacific cooling response to recent
567 Australian wildfires in CESM2, Science Advances, 9, eadg1213, 2023.

568 Flannigan, M. D., Krawchuk, M. A., de Groot, W. J., Wotton, B. M., and Gowman, L. M.: Implications of
569 changing climate for global wildland fire, International journal of wildland fire, 18, 483-507, 2009.

570 Flannigan, M. D., Logan, K. A., Amiro, B. D., Skinner, W. R., and Stocks, B.: Future area burned in Canada,
571 Climatic change, 72, 1-16, 2005.

572 Gelaro, R., McCarty, W., Suarez, M. J., Todling, R., Molod, A., Takacs, L., Randles, C. A., Darmenov, A.,
573 Bosilovich, M. G., Reichle, R., Wargan, K., Coy, L., Cullather, R., Draper, C., Akella, S., Buchard, V.,
574 Conaty, A., da Silva, A. M., Gu, W., Kim, G. K., Koster, R., Lucchesi, R., Merkova, D., Nielsen, J. E.,
575 Partyka, G., Pawson, S., Putman, W., Rienecker, M., Schubert, S. D., Sienkiewicz, M., and Zhao, B.: The
576 Modern-Era Retrospective Analysis for Research and Applications, Version 2 (MERRA-2), J Climate, 30,
577 5419-5454, 10.1175/Jcli-D-16-0758.1, 2017.

578 Giglio, L., Randerson, J. T., and Werf, G. R.: Analysis of daily, monthly, and annual burned area using the
579 fourth‐generation global fire emissions database (GFED4), Journal of Geophysical Research:
580 Biogeosciences, 118, 317-328, 2013.

581 Gillett, N., Weaver, A., Zwiers, F., and Flannigan, M.: Detecting the effect of climate change on Canadian
582 forest fires, Geophysical Research Letters, 31, 2004.

583 Harris, I., Jones, P., Osborn, T., and Lister, D.: Updated high‐resolution grids of monthly climatic
584 observations‐the CRU TS3. 10 Dataset, International Journal of Climatology, 34, 623-642, 2014.

585 Hersbach, H., Bell, B., Berrisford, P., Hirahara, S., Horanyi, A., Munoz-Sabater, J., Nicolas, J., Peubey, C.,
586 Radu, R., Schepers, D., Simmons, A., Soci, C., Abdalla, S., Abellan, X., Balsamo, G., Bechtold, P., Biavati,
587 G., Bidlot, J., Bonavita, M., De Chiara, G., Dahlgren, P., Dee, D., Diamantakis, M., Dragani, R., Flemming,
588 J., Forbes, R., Fuentes, M., Geer, A., Haimberger, L., Healy, S., Hogan, R. J., Holm, E., Janiskova, M.,
589 Keeley, S., Laloyaux, P., Lopez, P., Lupu, C., Radnoti, G., de Rosnay, P., Rozum, I., Vamborg, F.,
590 Villaume, S., and Thepaut, J. N.: The ERA5 global reanalysis, Quarterly Journal of the Royal
591 Meteorological Society, 146, 1999-2049, 10.1002/qj.3803, 2020.

592 Huang, X., Ding, K., Liu, J. Y., Wang, Z. L., Tang, R., Xue, L., Wang, H. K., Zhang, Q., Tan, Z. M., Fu,
593 C. B., Davis, S. J., Andreae, M. O., and Ding, A. J.: Smoke-weather interaction affects extreme wildfires
594 in diverse coastal regions, Science, 379, 457-461, 10.1126/science.add9843, 2023.

595 Huffman, G. J., Bolvin, D. T., Nelkin, E. J., and Tan, J.: Integrated Multi-satellitE Retrievals for GPM
596 (IMERG) technical documentation, Nasa/Gsfc Code, 612, 2019, 2015.

597 Huffman, G. J., Bolvin, D. T., Braithwaite, D., Hsu, K.-L., Joyce, R. J., Kidd, C., Nelkin, E. J., Sorooshian,
598 S., Stocker, E. F., and Tan, J.: Integrated multi-satellite retrievals for the global precipitation measurement
599 (GPM) mission (IMERG), Satellite Precipitation Measurement: Volume 1, 343-353, 2020.

600 Ichoku, C., Ellison, L. T., Willmot, K. E., Matsui, T., Dezfuli, A. K., Gatebe, C. K., Wang, J., Wilcox, E.
601 M., Lee, J., and Adegoke, J.: Biomass burning, land-cover change, and the hydrological cycle in Northern
602 sub-Saharan Africa, Environmental Research Letters, 11, 095005, 2016.

603 Jiang, Y. Q., Yang, X. Q., Liu, X. H., Qian, Y., Zhang, K., Wang, M. H., Li, F., Wang, Y., and Lu, Z.:
604 Impacts of Wildfire Aerosols on Global Energy Budget and Climate: The Role of Climate Feedbacks, J
605 Climate, 33, 3351-3366, 10.1175/Jcli-D-19-0572.1, 2020.

606 Jolly, W. M., Cochrane, M. A., Freeborn, P. H., Holden, Z. A., Brown, T. J., Williamson, G. J., and
607 Bowman, D. M. J. S.: Climate-induced variations in global wildfire danger from 1979 to 2013, Nature
608 Communications, 6, ARTN 753710.1038/ncomms8537, 2015.

609 Kanamitsu, M., Ebisuzaki, W., Woollen, J., Yang, S.-K., Hnilo, J., Fiorino, M., and Potter, G.: NCEP–DOE
610 AMIP-II Reanalysis (R-2), B Am Meteorol Soc, 83, 1631-1644, 2002.

611 Knorr, W., Dentener, F., Lamarque, J. F., Jiang, L. W., and Arneth, A.: Wildfire air pollution hazard during
612 the 21st century, Atmos Chem Phys, 17, 9223-9236, 10.5194/acp-17-9223-2017, 2017.

613 Koster, R. D., Darmenov, A. S., and da Silva, A. M.: The quick fire emissions dataset (QFED):
614 Documentation of versions 2.1, 2.2 and 2.4, 2015.

615 Kreidenweis, S. M., Remer, L. A., Bruintjes, R., and Dubovik, O.: Smoke aerosol from biomass burning in
616 Mexico: Hygroscopic smoke optical model, Journal of Geophysical Research: Atmospheres, 106, 4831-
617 4844, 2001.

618 Lee, Y. S., Collins, D. R., Li, R., Bowman, K. P., and Feingold, G.: Expected impact of an aged biomass
619 burning aerosol on cloud condensation nuclei and cloud droplet concentrations, Journal of Geophysical
620 Research: Atmospheres, 111, 2006.

621 Liu, Y. W., Zhang, K., Qian, Y., Wang, Y. H., Zou, Y. F., Song, Y. J., Wan, H., Liu, X. H., and Yang, X.
622 Q.: Investigation of short-term effective radiative forcing of fire aerosols over North America using nudged
623 hindcast ensembles, Atmos Chem Phys, 18, 31-47, 10.5194/acp-18-31-2018, 2018.

624 Lu, Z., Liu, X., Zhang, Z., Zhao, C., Meyer, K., Rajapakshe, C., Wu, C., Yang, Z., and Penner, J. E.:
625 Biomass smoke from southern Africa can significantly enhance the brightness of stratocumulus over the
626 southeastern Atlantic Ocean, Proceedings of the National Academy of Science, 201713703, 2018.

627 Magi, B., Rabin, S., Shevliakova, E., and Pacala, S.: Separating agricultural and non-agricultural fire
628 seasonality at regional scales, Biogeosciences, 9, 3003, 2012.

629 Marlon, J. R., Bartlein, P. J., Carcaillet, C., Gavin, D. G., Harrison, S. P., Higuera, P. E., Joos, F., Power,
630 M., and Prentice, I.: Climate and human influences on global biomass burning over the past two millennia,
631 Nature Geoscience, 1, 697-702, 2008.

632 Mouillot, F. and Field, C. B.: Fire history and the global carbon budget: a 1× 1 fire history reconstruction
633 for the 20th century, Global Change Biology, 11, 398-420, 2005.

634 Page, S. E., Siegert, F., Rieley, J. O., Boehm, H. D. V., Jaya, A., and Limin, S.: The amount of carbon
635 released from peat and forest fires in Indonesia during 1997, Nature, 420, 61-65, 10.1038/nature01131,
636 2002.

637 Pechony, O. and Shindell, D.: Fire parameterization on a global scale, Journal of Geophysical Research:
638 Atmospheres, 114, 2009.

639 Perdigon-Morales, J., Romero-Centeno, R., Barrett, B. S., and Ordonez, P.: Intraseasonal Variability of
640 Summer Precipitation in Mexico: MJO Influence on the Midsummer Drought, J Climate, 32, 2313-2327,
641 10.1175/Jcli-D-18-0425.1, 2019.

642 Power, M. J., Marlon, J., Ortiz, N., Bartlein, P. J., Harrison, S. P., Mayle, F. E., Ballouche, A., Bradshaw,
643 R. H., Carcaillet, C., and Cordova, C.: Changes in fire regimes since the Last Glacial Maximum: an
644 assessment based on a global synthesis and analysis of charcoal data, Climate dynamics, 30, 887-907, 2008.

645 Prasad, V. K., Badarinath, K., and Eaturu, A.: Biophysical and anthropogenic controls of forest fires in the
646 Deccan Plateau, India, Journal of Environmental Management, 86, 1-13, 2008.

647 Randerson, J., Chen, Y., Werf, G., Rogers, B., and Morton, D.: Global burned area and biomass burning
648 emissions from small fires, Journal of Geophysical Research: Biogeosciences, 117, 2012.

649 Rogers, C. M. and Bowman, K. P.: Transport of smoke from the Central American fires of 1998, Journal
650 of Geophysical Research: Atmospheres, 106, 28357-28368, 2001.

651 Running, S., Q. Mu, M. Zhao. : MODIS/Terra Gross Primary Productivity 8-Day L4 Global 500m SIN
652 Grid V061,distributed by NASA EOSDIS Land Processes Distributed Active Archive Center,
653 https://doi.org/10.5067/MODIS/MOD17A2H.061. Accessed 2023-12, 2021.

654 Tosca, M., Randerson, J., Zender, C., Flanner, M., and Rasch, P. J.: Do biomass burning aerosols intensify
655 drought in equatorial Asia during El Nino?, Atmospheric Chemistry and Physics, 10, 3515-3528, 2010.

656 Tosca, M. G., Randerson, J. T., and Zender, C. S.: Global impact of smoke aerosols from landscape fires
657 on climate and the Hadley circulation, Atmos Chem Phys, 13, 5227-5241, 10.5194/acp-13-5227-2013,
658 2013.

659 van Marle, M. J. E., Kloster, S., Magi, B. I., Marlon, J. R., Daniau, A. L., Field, R. D., Arneth, A., Forrest,
660 M., Hantson, S., Kehrwald, N. M., Knorr, W., Lasslop, G., Li, F., Mangeon, S., Yue, C., Kaiser, J. W., and
661 van der Werf, G. R.: Historic global biomass burning emissions for CMIP6 (BB4CMIP) based on merging
662 satellite observations with proxies and fire models (1750-2015), Geosci Model Dev, 10, 3329-3357,
663 10.5194/gmd-10-3329-2017, 2017.

664 Veira, A., Lasslop, G., and Kloster, S.: Wildfires in a warmer climate: Emission fluxes, emission heights,
665 and black carbon concentrations in 2090–2099, Journal of Geophysical Research: Atmospheres, 121, 3195-
666 3223, 2016.

667 Vermote, E.: NOAA CDR Program: NOAA Climate Data Record (CDR) of AVHRR Leaf Area Index
668 (LAI) and Fraction of Absorbed Photosynthetically Active Radiation (FAPAR), Version 5, Version, 5,
669 NOAA National Centers for Environmental Information. , 2019.

670 Voulgarakis, A. and Field, R. D.: Fire influences on atmospheric composition, air quality and climate,
671 Current Pollution Reports, 1, 70-81, 2015.

672 Winker, D. M., Tackett, J. L., Getzewich, B. J., Liu, Z., Vaughan, M. A., and Rogers, R. R.: The global 3-
673 D distribution of tropospheric aerosols as characterized by CALIOP, Atmos Chem Phys, 13, 3345-3361,
674 10.5194/acp-13-3345-2013, 2013.

675 Yokelson, R., Urbanski, S., Atlas, E., Toohey, D., Alvarado, E., Crounse, J., Wennberg, P., Fisher, M.,
676 Wold, C., and Campos, T.: Emissions from forest fires near Mexico City, Atmos. Chem. Phys, 7, 5569-
677 5584, 2007.

678 Yokelson, R. J., Crounse, J., DeCarlo, P., Karl, T., Urbanski, S., Atlas, E., Campos, T., Shinozuka, Y.,
679 Kasputin, V., and Clarke, A.: Emissions from biomass burning in the Yucatan, Atmospheric Chemistry and
680 Physics, 9, 5785, 2009.

Yue, S., Zhu, J., Chen, S., Xie, Q., Li, W., Li, L., Ren, H., Su, S., Li, P., and Ma, H.: Brown carbon from biomass burning imposes strong circum-Arctic warming, One Earth, 5, 293-304, 2022.

Zhang, Y. W., Fan, J. W., Shrivastava, M., Homeyer, C. R., Wang, Y., and Seinfeld, J. H.: Notable impact of wildfires in the western United States on weather hazards in the central United States, P Natl Acad Sci USA, 119, ARTN e220732911910.1073/pnas.2207329119, 2022.

Zhong, Q. R., Schutgens, N., van der Werf, G., van Noije, T., Tsigaridis, K., Bauer, S. E., Mielonen, T., Kirkevag, A., Seland, O., Kokkola, H., Checa-Garcia, R., Neubauer, D., Kipling, Z., Matsui, H., Ginoux, P., Takemura, T., Le Sager, P., Remy, S., Bian, H. S., Chin, M., Zhang, K., Zhu, J. L., Tsyro, S. G., Curci, G., Protonotariou, A., Johnson, B., Penner, J. E., Bellouin, N., Skeie, R. B., and Myhre, G.: Satellite-based evaluation of AeroCom model bias in biomass burning regions, Atmos Chem Phys, 22, 11009-11032, 10.5194/acp-22-11009-2022, 2022.